Planet. Space Sci., Vol. 27, pp. 385–401

0032-0633/79/0401-0385$02.00/0

A DYNAMIC MODEL OF THE MESOSPHERE AND LOWER THERMOSPHERE

T. J. KENESHEA, S. P. ZIMMERMAN and C. R. PHILBRICK
Air Force Geophysics Laboratory (AFSC), Hanscom AFB, Massachusetts 01731, U.S.A.

(*Received in final form* 8 *August* 1978)

Abstract—A one-dimensional, time-dependent calculation which includes the dynamics of turbulence has been developed. The dynamical parameters together with the mass density and temperature structure measured during the ALADDIN I program are inputs to the calculations of the vertical distribution of [O], [O_2], [$O_2(^1\Delta_g)$], [OH] and [Ar] between 50 and 150 km. The results of the calculations are compared with measurements of these species distributions made during the ALADDIN I program and are also related to reported results at other times. Good to excellent agreement is found when the calculated profiles are compared with the measurements. This agreement supports the contention of the authors that the turbulent parameters measured from chemical trail fluctuations are due to atmospheric turbulence and are appropriate for use in model calculations. Significant changes in species concentrations occur when the eddy diffusion coefficient is increased. In particular, an increase in molecular oxygen and a reduction in atomic oxygen and helium are noted.

INTRODUCTION

Many authors have reported investigations of the chemical and transport processes that cause the complex inter-relations among the atmospheric species of the mesosphere and lower thermosphere. While the general chemistry and motions affecting the major and minor atmospheric constituents are semi-quantitatively known, the specifics of transport and chemistry have never been tested by measurement except in a general manner. It was towards this end that measurements of *in situ* transport parameters were incorporated into a one-dimensional chemical-transport model calculation. The subsequent comparison of the profiles developed in these calculations with measured major and minor species distributions, determined simultaneously with the mass density, temperature and the transport parameters, was the basis upon which the ALADDIN I experiment was conceived and executed on 20 November 1970 from Eglin AFB, Florida (Rosenberg *et al.*, 1973; Philbrick *et al.*, 1973a).

It has been known for many years that the atomic oxygen produced from the dissociation of molecular oxygen by solar ultra violet radiation above 95 km must be transported downward by a process more effective than molecular diffusion in order to supply the atomic oxygen required for the three body recombination processes in the more dense atmosphere. This dominant transport mechanism for all regions below about 100 km has been referred to previously by several authors as eddy mixing, eddy diffusion, turbulent diffusivity, or eddy transport. Models covering the region above 120 km, which is controlled mainly by molecular scale diffusive processes, have been developed on an empirical basis to give fairly realistic values of atmospheric density (i.e., Jacchia, 1971) but are not satisfactory for inferring atmospheric composition nor for understanding the influence of the various physical processes. Over the past decade several efforts have progressively developed towards a physically realistic atmospheric model that includes measured solar fluxes, laboratory measurements of the cross-sections for absorption and photodissociation, measured chemical reaction rate coefficients, and various representations of the dyamical processes that are important in transporting the species.

The first major step in handling the dynamical considerations was the introduction of the concept of eddy diffusion into calculations of atmospheric species distributions (Lettau, 1951; Colegrove *et al.*, 1965, 1966). Colegrove *et al.*, determined the vertical distribution of the major atmospheric species using a constant eddy diffusion profile and compared the atomic to molecular oxygen ratio with the value of near unity at 120 km as measured by early mass spectrometers. Estimates of the average effective value of a constant eddy diffusion coefficient of between 10^6 and 10^7 cm^2 s^{-1} were found to be acceptable in these studies.

A second major step in the development of physical models was the solution of the time-dependent equations of motion and continuity by Shimazaki (1967). This calculation was made assuming that the solar flux was continuously impinging upon the atmosphere and used an eddy diffusion coefficient that

was constant with altitude. The computed atomic oxygen distribution was found to reach an asymptotic solution after about 20 simulated days. The results provided a fairly consistent view of the effects of transport upon the distribution of atomic oxygen with an assumed constant eddy diffusion coefficient of about 10^7 cm^2 s^{-1}. Calculations using a constant eddy diffusion coefficient, though physically unrealistic, do illustrate the important effects produced when transport processes are included in atmospheric models.

The third major step was the inclusion of a realistic shape function for the altitude dependence of the eddy diffusion coefficient and the inclusion of the diurnal variation of the solar flux (Hesstvedt, 1968; Keneshea and Zimmerman, 1970). The calculations of Hesstvedt provided valuable insight into the effects of dynamical transport on the species profiles. The calculations of Keneshea and Zimmerman incorporated measured turbulent diffusion coefficients and demonstrated good agreement with the then available measurements of atmospheric constituents. Additional investigations have advanced our understanding of the effects that various assumptions about the dynamic processes and the boundary values have on such calculations (Shimazaki and Laird, 1970; George *et al.*, 1972; Strobel, 1972).

The experimental program for measuring species distributions and transport parameters pertinent to these calculations has already been described (Philbrick *et al.*, 1973a). It is the purpose of this paper to present the equations of state, the applicable chemistry and transport relations and the comparison of the theoretical species profiles with those measured. The atmospheric species included in the model are O, O_2, O_3, OH, H, H_2, HO_2, H_2O, $O(^1D)$, $O_2(^1\Delta_g)$, He and Ar with N_2 as the time invariant background gas. The model covers the altitude region from 50 to 400 km. However, only the results between 50 and 150 km will be discussed here.

TRANSPORT PARAMETERS

The calculations utilize the minimum vertical turbulent diffusivity determined from the study of the variance and spectra of the fluctuations exhibited in the photographs of the chemical release (Zimmerman and Trowbridge, 1973). From this study, the wind system at the time of the experiment (Rosenberg *et al.*, 1973) was also obtained. However, since there has been so much controversy over the question of what turbulent diffusion coefficients are correct for use in calculations of this type, a short review of previous measurements, estimates and assumptions are worthwhile at this point.

Hunten and Strobel (1974) have presented a discussion of some of the eddy diffusion coefficients used by modelers. We shall review some of their arguments on this topic, discuss some additional analyses not covered by them, and then briefly reiterate some features of the derived diffusivities used in these calculations.

Hunten and Strobel (1974) question the assumption of Keneshea and Zimmerman (1970) that turbulence is isotropic over the scales measured in the horizontal analysis of the turbulence exhibted in photographs of chemical releases. However, they do not examine what values would be reasonable for these stably limited scales in this region. In isotropic homogeneous flow, the parameter describing the transfer of turbulent kinetic energy from the large energy-bearing scales to those limited by kinematic viscosity is the rate of dissipation of turbulent kinetic energy, ε, which is constant in the inertial subrange of the energy spectrum. It has been amply demonstrated in turbulence measurements in the mesosphere and in the lower thermosphere (Zimmerman and Trowbridge, 1973) that the observed spectrum does, indeed, follow Kolmogoroff's law for this inertial condition; i.e., $E(k) \sim \varepsilon^{2/3} k^{-5/3}$, where $E(k)$ is the spectral energy density and k is the wavenumber. Then following Lumley (1964) and Phillips (1967), it can be shown that in a stably stratified atmosphere the vertical component of the spectrum will be "inertial" to a scale size given by $l_B = C_1(\varepsilon/N^3)^{1/2}$ where N is the Brunt Väisälä frequency defined as $N^2 = g/T(\partial T/\partial z + \Gamma)$, Γ being the adiabatic lapse rate $\simeq 10$ K/km. For arguments sake, let us assume that the constant of proportionality $C_1 = 1$. Then, using values for the rate of dissipation of 10^3 to 10^5 cm^2/s^3 (Zimmerman and Trowbridge, 1973) and $N \simeq 2 \times 10^{-2}$ s^{-1} in the expression l_B, we have $\sim 100 < l_B <$ 1000 m. These values are within the limits discussed by Keneshea and Zimmerman (1970) and support their assumption of isotropy in arriving at their values of diffusivity.

The minimum turbulent diffusion coefficients determined from the observations on chemical trails (Zimmerman and Trowbridge, 1973) are displayed in Fig. 1. The profile shows several sharp turbulent layers rather than the single broad layer used by Keneshea and Zimmerman (1970). The vertical turbulent diffusion coefficients above 94 km are based upon measurements of the rate of dissipation of turbulent kinetic energy (Zimmerman and Trowbridge, 1973) and the stability criterion determined from the simultaneously measured temperature profile of Theon and Horvath (1972). Below the altitude at which the measurements begin, the curve is chosen to follow an exponential that closely resembles the turbulent heat

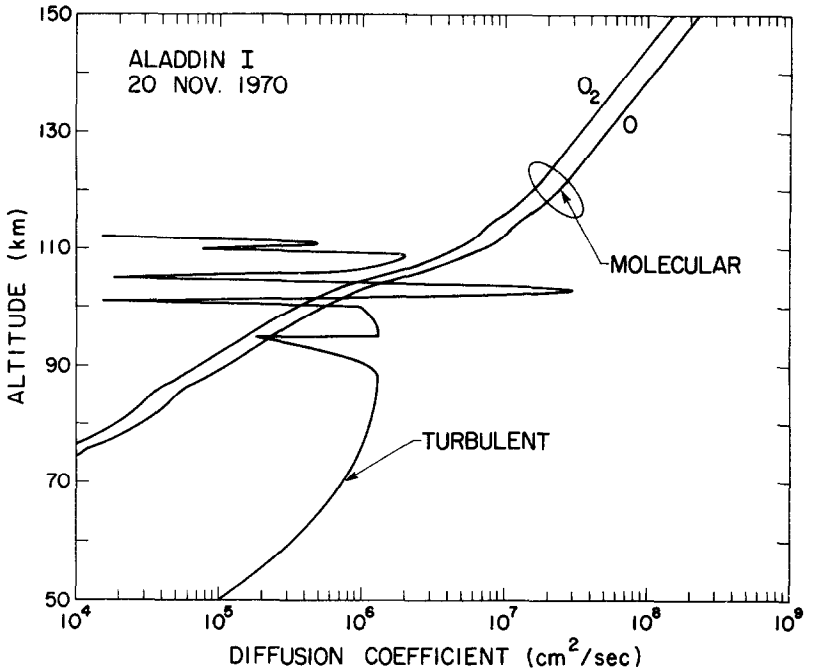

FIG. 1. DIFFUSION COEFFICIENTS.

The curve labeled TURBULENT represents the eddy diffusion coefficients determined from the chemical release data obtained from the ALADDIN I experiments.
The curves labeled O and O_2 are the molecular diffusion coefficients for these species computed from equation (6).

transfer calculations of Johnson and Wilkins (1965) and has a value of $1\times10^5\,cm^2\,s^{-1}$ at 50 km as measured by Beaudoin *et al.* (1967). When comparing the heat transfer calculations, which represent an upper limit to the turbulent diffusion coefficients, with the upper part of the measured profile, one should realize that such a structured profile may not be at all inconsistent with the average heat transfer represented in those calculations. Indeed, some of the earlier reported large values (Zimmerman and Champion, 1963) may represent points on such structured profiles rather than effective average parameters. It should be re-emphasized here that the data labeled K are minimal vertical turbulent diffusivities which have been determined from the measurement of the rate of dissipation of turbulent kinetic energy and the smallest length scale of the buoyantly damped turbulent motions. It is not known to what extent the buoyant sub-range will go into the lower wave number region, but it is obvious that there must be a continuous transfer of energy from the shear source to the inertial range. The unknown here is the separation between the source range and the isotropic inertial range. Since this region of the buoyance sub-range must contribute to increase the turbulent diffusivity, the calculations are made for the cases K and $3K$. Examination of Fig. 1 shows what is apparently an inconsistency in that the molecular diffusion coefficient for O_2 is larger than the upper peak of the turbulent diffusion coefficient, K. This situation might exist in decaying turbulence, but for the models that hypothesize this turbulent diffusivity as constant with time, it can be argued that this is incorrect. However, it should be remembered that this is the minimum theoretical diffusivity based upon measurements of the rate of dissipation (ε) and the Brunt-Väisälä frequency (N). The real turbulent transfer coefficient should be larger than this minimum as estimated by the use of $3K$. In these calculations, the peaks of turbulent diffusivity have arbitrarily been allowed to exist for $K < D_{O_2}$ even though there is argument (above) to remove them. We feel that their existence will not produce significant differences in the calculations.

EQUATIONS OF STATE

The equation of conservation of particles, the continuity equation, for a given gas species is

$$\frac{\partial n_i}{\partial t} = F_i - n_i R_i - \nabla \cdot \mathbf{\Phi}_i \tag{1}$$

where n_i is the concentration of species i, F_i is the rate at which the species is chemically formed, $n_i R_i$ is the rate at which it is chemically removed and $\mathbf{\Phi}_i$ is the vector flux of the species induced by all non-chemical processes. For the purposes of this work, only one dimensional vertical molecular and eddy diffusion will be considered in the flux term:

$$\mathbf{\Phi}_i = n_i \mathbf{C}_i + n_i \mathbf{V}_i \tag{2}$$

where $\mathbf{C}_i$ is the velocity of species $_i$ resulting from molecular diffusion and $\mathbf{V}_i$ is the velocity resulting from eddy diffusion. Thus the continuity equation becomes:

$$\frac{\partial n_i}{\partial t} = F_i - n_i R_i - \frac{\partial}{\partial z}(n_i C_i + n_i V_i). \tag{3}$$

For a minor species diffusing through a fixed background gas of much higher concentration the equation of motion can be written as (Chapman and Cowling, 1970; Shimazaki, 1967; Keneshea and Zimmerman, 1970):

$$\frac{\partial C_i}{\partial t} = \frac{kT}{m_i}\left[\frac{C_i}{D_i} + \frac{1}{n_i}\frac{\partial n_i}{\partial z} + \frac{(1+\alpha_i)}{T}\frac{\partial T}{\partial z} + \frac{1}{H_i}\right] \tag{4}$$

where k is Boltzmann's constant, T the temperature, m_i the mass, α_i the thermal diffusion factor and H_i the scale height of the i^{th} species. The molecular diffusion coefficient of species i in a multi-component gas is given by

$$D_i = \frac{1}{\sum_j \frac{x_j}{D_{ij}}} \tag{5}$$

where $x_j = n_j/N$, the mixing ratio of the j^{th} species.

The molecular diffusion coefficients for a binary gas are computed using the approximation of Chapman and Cowling (1970) for rigid elastic spheres of diameters σ_i and σ_j

$$D_{ij} = \frac{3}{8N\sigma_{ij}^2}\left\{\frac{kT(m_i+m_j)}{2\pi m_i m_j}\right\}^{1/2} \tag{6}$$

where $\sigma_{ij} = \frac{1}{2}(\sigma_i + \sigma_j)$, N is the total concentration and m_j is the mass of fixed background gas (N_2).

The thermal diffusion factors are assumed to be zero except for the following species: O(−0.27), H(−0.39), H_2(−0.31) and He(−0.36) (Zimmerman and Keneshea, 1976).

The eddy diffusion velocity, taken from the formulation of Colegrove *et al.* (1966) is

$$V_i = -K\left[\frac{1}{n_i}\frac{\partial n_i}{\partial z} + \frac{1}{T}\frac{\partial T}{\partial z} + \frac{1}{H_m}\right] \tag{7}$$

where K is the eddy diffusion coefficient and H_m is the scale height of the mean molecular mass.

Writing 3, 4, and 7 in a finite difference notation and combining them leads to an equation for each species of the following form which can be solved at each altitude point z, for the concentration at time $t + \Delta t$.

$$-A_z^t n_{z+\Delta z}^{t+\Delta t} + B_z^t n_z^{t+\Delta t} - C_z^t n_{z-\Delta z}^{t+\Delta t} = D_z^t \tag{8}$$

where the coefficients A_z^t, B_z^t, C_z^t and D_z^t can be evaluated from known quantities at time t.

The tridiagonal set of equations (8) are solved subject to appropriate boundary conditions by the method of Richtmyer and Morton (1967).

INITIAL CONDITIONS

The temperature (Fig. 2) and mass density in the region 50–125 km are taken from the measurements of Theon and Horvath (1972). From 125–160 km the measurements of these parameters by Golomb (Rosenberg *et al.*, 1973) are used. Above 160 km, the values are taken from the 900K exospheric temperature winter model of the U.S. Standard Atmosphere Supplements, 1966. The initial values of the mean molecular weight of the atmosphere are fixed at 28.96 up to 80 km. Above 80 km, the initial values of the mean molecular weight are taken from the winter model of the U.S. Standard Atmosphere Supplements, 1966.

Initial height profiles of all the species are required for the solution of the finite difference equations. From the lower boundary up to the turbopause, the altitude above which turbulence ceases to exist, the total concentration at each altitude point is computed from the measured mass density (ρ), and the initial mean molecular weights, $\bar{m}$, (i.e., $N = \rho/\bar{m}$). Below the turbopause each of the species is assumed to be completely mixed so that its concentration at any altitude is simply the product of the total concentration and its mixing ratio. A mixing ratio of 5 ppmv for water vapor is assumed. Above the turbopause each species is assumed to be in diffusive equilibrium which permits its concentration to be computed from the hydrostatic equation

$$\frac{1}{n_i}\frac{\partial n_i}{\partial z} + \frac{(1+\alpha_i)}{T}\frac{\partial T}{\partial z} + \frac{1}{H_i} = 0. \tag{9}$$

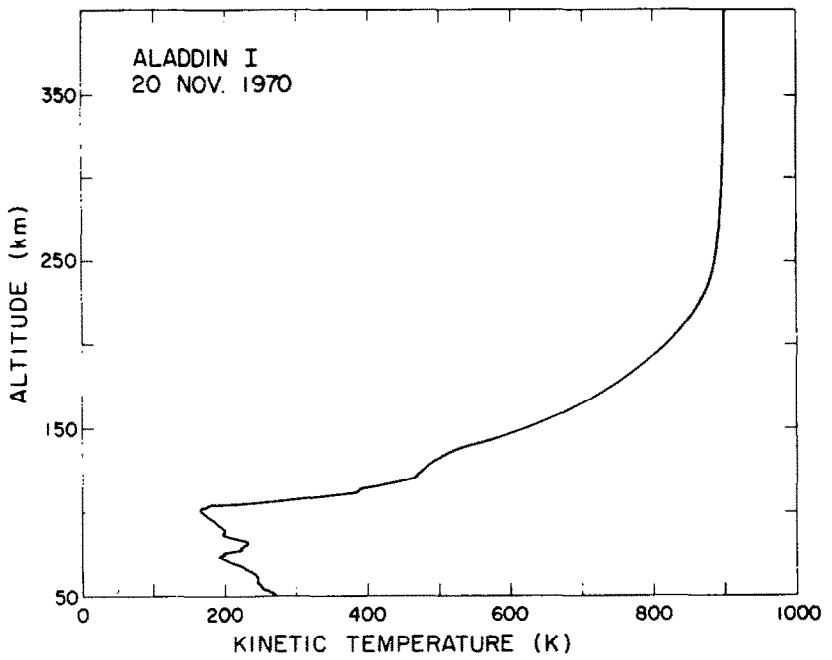

FIG. 2. THE STATIC TEMPERATURE PROFILE.
The values from 50 to 125 km are the measurements of Theon and Harvath (1972). The values from 125 to 160 km are the measurements of Golomb (Rosenberg *et al.*, 1973). Both of these measurements were made in the ALADDIN I program.

The analytical solution of (9) is

$$n_i = n_{io}\left(\frac{T_o}{T}\right)^{(1+\alpha_i)} \exp\left[-\frac{m_i}{k}\int_{z_o}^{z}\frac{g}{T}\,dz\right] \qquad (10)$$

where g is the acceleration of gravity and the subscript zero indicates values at the turbopause.

The argon concentrations are fixed throughout the time-dependent calculations. Its profile is computed assuming that its net velocity throughout the volume is zero ($C_{Ar} + V_{Ar}) = 0$, and also that

$$\frac{\partial C_{Ar}}{\partial t} = 0.$$

Then, using (4) and (7), the analytical solution for the vertical profile of argon is

$$n_{Ar} = (n_{Ar})_o\left(\frac{T_o}{T}\right) \times \exp\left[-\frac{1}{k}\int_{z_o}^{z}\left(\frac{m_{Ar}D_{Ar} + \bar{m}K}{D_{Ar} + K}\right)\frac{g}{T}\,dz\right] \qquad (11)$$

where D_{Ar} is the molecular diffusion coefficient for argon. It has been found that the neutral profiles described by complete mixing up to the turbopause and diffusive equilibrium above do not represent satisfactory initial conditions for starting the time-dependent solutions. In order to reduce the amount of computer time for the time-dependent solution to overcome these initial conditions, these profiles are used to solve the steady-state equations that result from setting the time derivatives in (3) and (4) to zero. The steady-state equations are solved using solar conditions corresponding to three hours after local noontime. The profiles resulting from the steady-state solution are then used as initial conditions for the time-dependent solution. The time-dependent calculations are started at noon and solutions are continued until all species reproduced their concentrations diurnally at all altitudes to within one per cent. This condition of diurnal reproducibility is generally arrived at after about 25 solution days.

HEIGHT STEP CONSIDERATIONS

In the early stages of the model calculations, a height step of 1 km was used. It was found, however, that the profile obtained for argon from the solution of the finite difference equations was considerably different from that computed from the analytical relation (11). The difference between the two solutions was attributed to the fact that the 1 km height step used in the finite difference solution was too large to accurately describe the vertical gradients. The height

increment in the finite difference solution had to be reduced to 100 m before the two solutions coincided.

In order to reduce the amount of core storage required as well as the amount of computer time per solution, a variable height step array was used. From the lower boundary, 50 km, up to 90 km the height step was fixed at 100 m. From 90 to 400 km the height step was computed by assuming that it was proportional to the pressure scale height of the atmosphere. This produced a height array with 940 grid points with a maximum height step at the upper boundary of about 1.25 km and showed no difference in the argon profile from that obtained with the constant 100 m height steps.

BOUNDARY CONDITIONS

The solution of the steady-state as well as the time-dependent finite difference equations requires the specification of lower and upper boundary conditions. At the lower boundary, the concentrations of O_2, H_2O, H_2 and He, are held fixed at their mixed values throughout the time-dependent calculations. All other species prove to be chemically controlled at the lower boundary so their concentrations are computed from chemistry only. For each of these species, the height derivative in (3) is set to zero and the resulting ordinary differential equation is solved for the time-dependent lower boundary concentrations. At the upper boundary, the velocity of each species is assumed to be zero with the exception of atomic hydrogen and helium. From Banks and Kockarts (1973) the efflux velocity of atomic hydrogen, at 400 km and an exospheric temperature of 900 K, is calculated to be 346 cm s^{-1}. The efflux velocity of helium is arbitrarily taken to be 1 cm s^{-1}.

CHEMISTRY

The chemical reactions operating in the model and their rate coefficients are given in Table 1. The intensity of the solar flux in the wavelength interval

TABLE 1. THE CHEMICAL REACTION SCHEME USED IN THE MODEL. THE RATE COEFFICIENTS FOR THE PHOTODISSOCIATION REACTIONS ARE DEPENDENT UPON THE SOLAR ZENITH ANGLE

Reaction	Rate coefficient	Reference
$O+O+M \rightarrow O_2+M$	$3\times10^{-33}\,(T/300)^{-2.9}$	Campbell and Thrush (1967)
$O+O_2+M \rightarrow O_3+M$	$5.5\times10^{-34}\,(T/300)^{-2.6}$	Kaufman and Kelso (1964)
$O+O_3 \rightarrow O_2+O_2$	$1.2\times10^{-11}\,e^{-(2000/T)}$	Schiff (1969)
$O+OH \rightarrow H+O_2$	2.2×10^{-11}	Baulch *et al.* (1972)
$O+HO_2 \rightarrow OH+O_2$	1×10^{-11}	Kaufman (1964)
$O+H_2 \rightarrow OH+H$	$7\times10^{-11}\,e^{-(5100/T)}$	Wong and Potter (1965)
$O+H_2O_2 \rightarrow OH+HO_2$	$1.4\times10^{-12}\,e^{-(2125/T)}$	Davis *et al.* (1974)
$O+H_2O_2 \rightarrow H_2O+O_2$	$1.4\times10^{-12}\,e^{-(2125/T)}$	Davis *et al.* (1974)
$O_3+H \rightarrow O_2+OH$	2.6×10^{-11}	Kaufman (1964)
$O_3+OH \rightarrow HO_2+O_2$	$1.3\times10^{-12}\,e^{-(950/T)}$	Anderson and Kaufman (1973)
$O_3+HO_2 \rightarrow OH+O_2+O_2$	$1\times10^{-13}\,e^{-(1250/T)}$	Garvin (1973)
$H+O_2+M \rightarrow HO_2+M$	$2.1\times10^{-32}\,e^{(300/T)}$	DNA Reaction Rate Handbook
$H+HO_2 \rightarrow H_2+O_2$	1.5×10^{-12}	Hunten and McElroy (1970)
$H+HO_2 \rightarrow OH+OH$	1×10^{-11}	Kaufman (1964)
$H+H_2O_2 \rightarrow H_2+HO_2$	$2.8\times10^{-12}\,e^{-(1900/T)}$	Baulch *et al.* (1972)
$OH+OH \rightarrow H_2O+O$	2×10^{-12}	Kaufman (1969)
$OH+HO_2 \rightarrow H_2O+O_2$	2×10^{-10}	Hochanadel *et al.* (1972)
$OH+H_2O_2 \rightarrow H_2O+HO_2$	$1.7\times10^{-11}\,e^{-(900/T)}$	Baulch *et al.* (1972)
$HO_2+HO_2 \rightarrow H_2O_2+O_2$	$3.0\times10^{-11}\,e^{-(500/T}$	Hampson *et al.* (1973)
$O(^1D)+O_3 \rightarrow O_2+O_2$	3×10^{-10}	Snelling and Bair (1967)
$O(^1D)+O_2 \rightarrow O+O_2$	5×10^{-11}	Young *et al.* (1968)
$O(^1D)+N_2 \rightarrow O+N_2$	5×10^{-11}	Young *et al.* (1968)
$O(^1D)+H_2O \rightarrow OH+OH$	3×10^{-10}	Garvin (1972)
$O(^1D)+H_2 \rightarrow OH+H$	1.9×10^{-10}	Young *et al.* (1968)
$O_2(^1\Delta_g)+O_3 \rightarrow O_2+O_3$	3×10^{-15}	Wayne and Pitts (1969)
$O_2(^1\Delta_g)+M \rightarrow O_2+M$	4.4×10^{-19}	Clark and Wayne (1969)
$O_2(^1\Delta_g) \rightarrow O_2$	2.58×10^{-4}	Badger *et al.* (1965)
$O_2(^1\Delta_g)+H \rightarrow OH+O$	2.5×10^{-14}	Schmidt and Schiff (1973)
$O_2+h\nu \rightarrow O+O$	$1750<\lambda<2424$ Å	
$O_2+h\nu \rightarrow O(^1D)+O$	$\lambda<1750$ Å	
$O_3+h\nu \rightarrow O_2(^1\Delta_g)+O(^1D)$	$\lambda<3100$ Å	
$O_3+h\nu \rightarrow O_2+O$	$3100<\lambda<7300$ Å	
$H_2O+h\nu \rightarrow OH+H$	$1219<\lambda<1864$ Å	
$H_2O_2+h\nu \rightarrow OH+OH$	$1882<\lambda<3030$ Å	

1163–7300 Å used in computing the photodissociation rate coefficients is taken from Ackerman (1971). These values of the solar flux in the Schumann–Runge continuum may be high by a factor of approximately two (Heroux and Swirbalus, 1976). The effect of reducing the intensity in this band was considered by Keneshea and Zimmerman (1970) who showed that for a factor of two reduction of the Schumann–Runge continuum there was a reduction of the atomic oxygen concentration by almost this same factor, accompanied by an increase of molecular oxygen. The absorption cross-sections as a function of wavelength for O_2 and O_3 are those compiled by Ackerman (1971). In the region of the Schumann–Runge bands of O_2 the measurements of Hudson and Mahle (1972) are used. The absorption cross-sections for water vapor and hydrogen peroxide are those reported by Watanabe and Zelikoff (1953) and Volman (1963), respectively.

RESULTS

As mentioned previously, the calculations were performed for each turbulent diffusion profile K and $3K$. This was done in order to ascertain the correspondence between the theoretical species profiles and those measured in the ALADDIN I program.

The measurement of argon is very important to this program because it is a chemically inert species so it responds only to transport effects. Thus, argon is a good indicator of the validity of the transport coefficients measured, particularly the turbulent diffusion coefficient. To compare theory with the measurement, the argon to nitrogen ratio relative to the ground-based Ar/N_2 ratio is plotted in Fig. 3. It is obvious that the theory using the K and $3K$ turbulent diffusivities quite accurately predicts the distribution of the measured Ar/N_2 ratio. From this, we may infer that the turbulent intensities and, in particular, the vertical distribution of turbulence, as revealed by chemical trails, is appropriate for these model calculations. It is

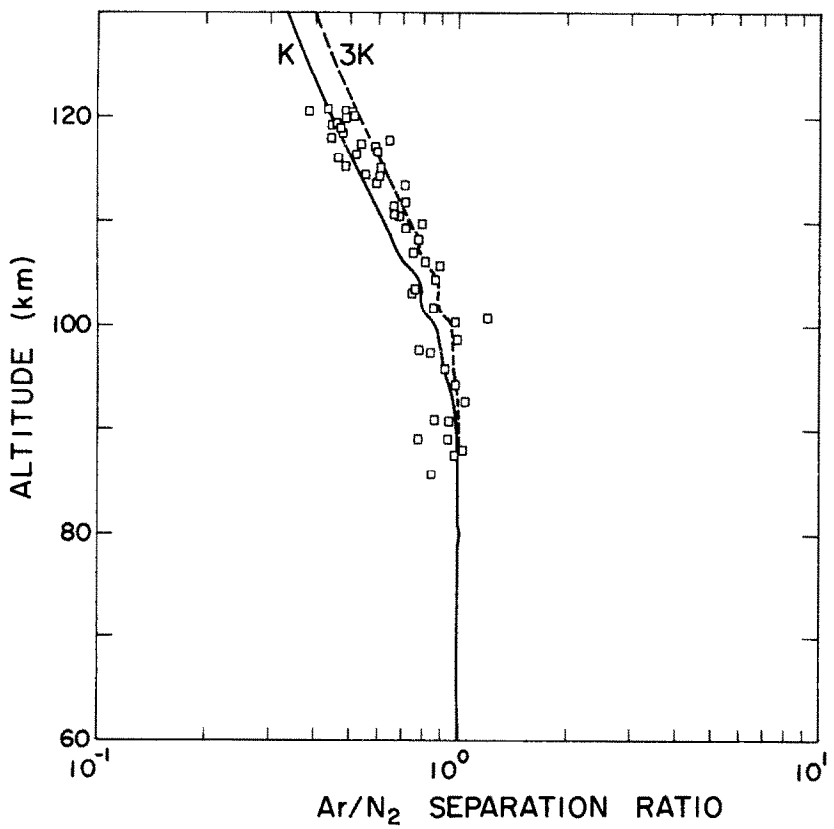

FIG. 3. THE ARGON TO NITROGEN SEPARATION RATIO.
The solid profile is the computed values for the turbulent diffusion coefficients K and the dashed profile is the computed values for the turbulent diffusion coefficients $3K$. The squares represent the measured ratios.

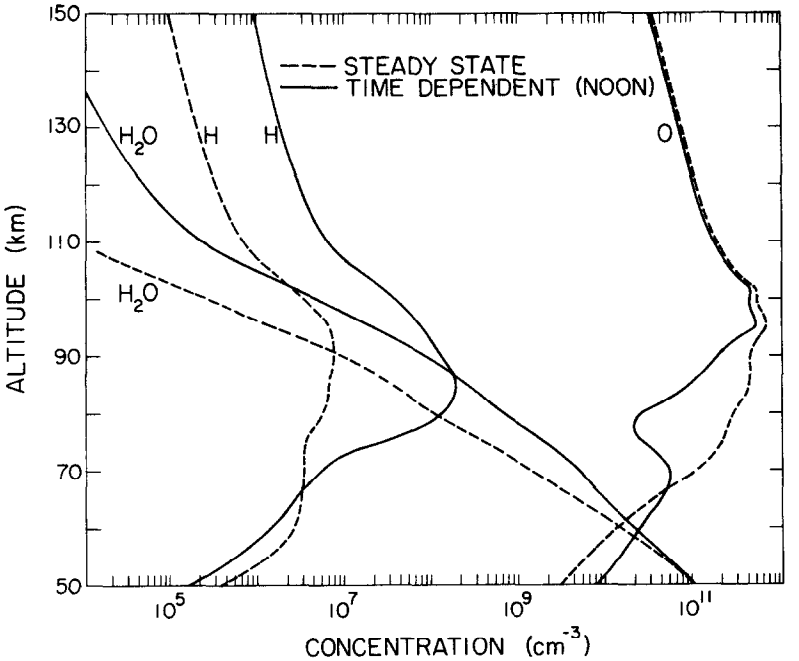

FIG. 4. THE STEADY-STATE PROFILES (DASHED CURVES) AND THE NOONTIME PROFILES (SOLID CURVES) TAKEN FROM THE LAST SOLUTION DAY OF THE TIME-DEPENDENT CALCULATIONS FOR THE SPECIES O, H AND H_2O.

of interest to note that the structure in the calculated Ar/N_2 profiles shows the effect that turbulent and laminar layers can create through alternate mixing and diffusive flows. It is also of interest to note that there appear to be coincident layers in the measurements. A point to remember is that these calculations are one-dimensional in the vertical.

Before discussing the data and calculations for the remainder of the measured species, let us consider the results of the initial steady-state calculations as compared with the time-dependent solution. The comparison is of interest because of the many calculations that have been and are being performed using only steady-state equations. The steady-state profiles of atomic oxygen, water vapor, and hydrogen do not accurately depict the distributions of these species in the upper mesosphere and thermosphere. The time-dependent calculations take into account the day–night changes that are important in most species distributions. Species such as atomic oxygen, atomic hydrogen and water vapor have regions of the atmosphere where they are strictly chemically dominated. In certain of these regions, the species concentration will shift markedly from the steady-state profile in the course of the time-dependent calculations. This is demonstrated in Fig. 4 which shows the mesosphere and lower thermosphere distributions of [O], [H] and $[H_2O]$ for steady-state and for noontime after reaching diurnal reproducibility. The difference is indeed significant, particularly in the mesosphere above 80 km which approximately marks the transition region from chemical to transport dominance.

THE ALADDIN RESULTS

In Fig. 5 the calculations are compared with the mass spectrometer measurements of N_2, O_2, O, Ar, and the $O_2(^1\Delta_g)$ photometer measurements (Philbrick *et al.*, 1973a) at a solar zenith angle of 98° during evening twilight. The computed profiles, as discussed earlier for the Ar/N_2 ratio, show very good agreement with measurements. The difference between the measured and calculated values for atomic oxygen can be attributed to the difficulty in measuring this highly reactive species and perhaps to the flux values used for the Schumann–Runge continuum. The Ackerman (1971) flux compilation may be a factor of ~2 too high, if some of the recent measurements of Heroux and Swirbalus (1976) are more accurate than those used by Ackerman. Generally, rocketborne mass spectrometer measurements tend to underestimate the atmospheric concentration of atomic oxygen (Lake and Nier, 1973; von Zahn, 1970) measured in the mesosphere and lower thermosphere. No correction for atomic oxygen loss processes have been applied to

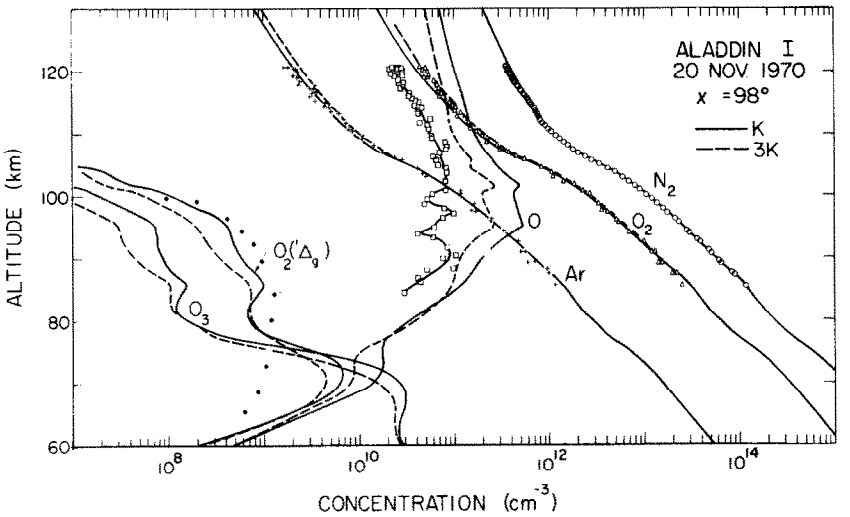

FIG. 5. COMPARISON OF COMPUTED SPECIES PROFILES FOR TURBULENT DIFFUSIVITIES K AND $3K$ (SOLID DASHED CURVES) WITH MEASURED PROFILES FOR O (SQUARES), O_2 (TRIANGLE), N_2 (CIRCLES), Ar (CROSSES) AND $O_2(^1\Delta_g)$(DOTS).

the data shown in Fig. 5. The 44 amu measurement corresponds well to the 16 amu profile above 95 km which shows some loss of atomic oxygen to the formation of CO_2. Below 95 km the 44 amu measurement shows that CO_2 is very near the ground level mixing ratio. The structure in the atomic oxygen profile is considerably larger than the relative profile error ($\sim \pm 15\%$ over most of the profile). The calculated profile also shows some structure which, although not in exact correspondence, indicates the effect that turbulent layers may have on the atomic oxygen distribution. A nearly identical instrument flown at another time did not exhibit the structure seen in this profile (Philbrick *et al.*, 1973b). The general agreement between the model above 70 km and the $O_2(^1\Delta_g)$ measurement tends to support the validity of the calculated profile of atomic oxygen in this region because of the photochemical reactions coupling the O, O_3 and $O_2(^1\Delta_g)$ concentrations. This is particularly true in this 98° post-sunset period where the $O_2(^1\Delta_g)$ concentration is changing very rapidly.

The noontime fluxes and the noontime and midnight production and loss rates between 50 and 150 km are shown in Figs. 6–8 for atomic oxygen. The noon values clearly follow contemporary thought in that the production and loss processes are chemically dominated in the mesosphere, and production and transport dominated in the thermosphere. The nighttime results for O_3, Fig. 9, show striking differences from these lines of thought. Ozone is transport dominated from 50 to ~75 km; however, in spite of this, the O_3 concentrations will show little change because of its large chemical and transport time constants in this region. An unexpected result of these calculations is the transport domination of hydrogen peroxide throughout the mesosphere. This species is most interesting in that the night-time profile results strictly from its production by HO_2 and transport redistribution. With convergent and divergent motions whose effective time constant is $\sim 10^4$ s, this species should exhibit strongly any of the fluctuations created by waves and turbulence in a manner similar to oxygen above ~75 km. Indeed, H_2O_2 appears to be a most effective tracer material unless there is some chemical reaction such as $Cl + H_2O_2$ not considered here that would affect its chemical loss time. Figures 10–14 display the mesospheric diurnal behavior of [O], [H], [O_3], [OH], and [$O_2(^1\Delta_g)$]. They show, within the constraints of the model, the expected diurnal variations of these species below 90 km. That they are similar in general to many other time-dependent calculations is also to be expected. The differences are primarily in the amplitudes at any given time and altitude and are due to the different transfer coefficients used in the calculations presented here.

Given the good to excellent agreement found between the calculated profiles and the measurements of the ALADDIN I program, we naturally turn to the comparison of the calculations with other recent measurements. Even though the temperature, density, and transport parameters used apply to the conditions at sunset on the day of the measurements,

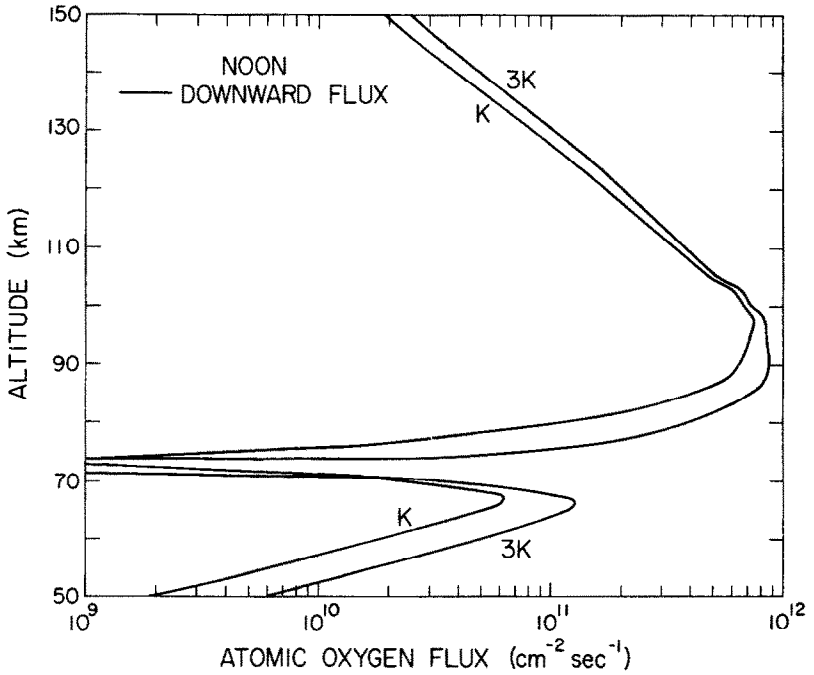

FIG. 6. THE NOONTIME FLUX OF ATOMIC OXYGEN FROM 50 TO 150 km.
Except for the small region above 70 km, the flux is everywhere downward.

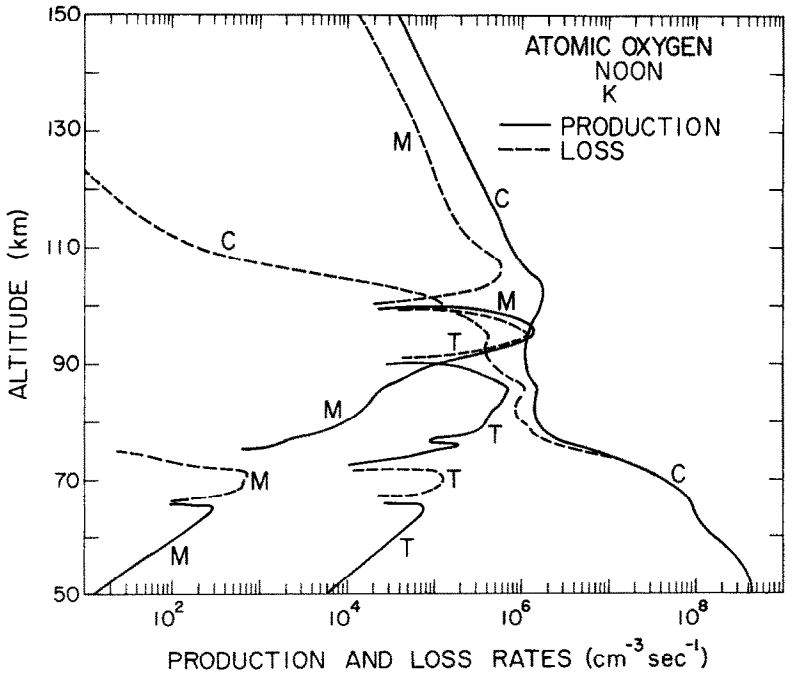

FIG. 7. COMPARISON OF THE PRODUCTION AND LOSS TERMS IN THE CONTINUITY EQUATION FOR ATOMIC OXYGEN AT NOON FOR THE TURBULENT DIFFUSIVITY K.

The curves labeled C represent the contributions of chemistry; those marked M represent the amplitude of the molecular flux gradient and those labeled T represent the amplitude of the turbulent flux gradient.

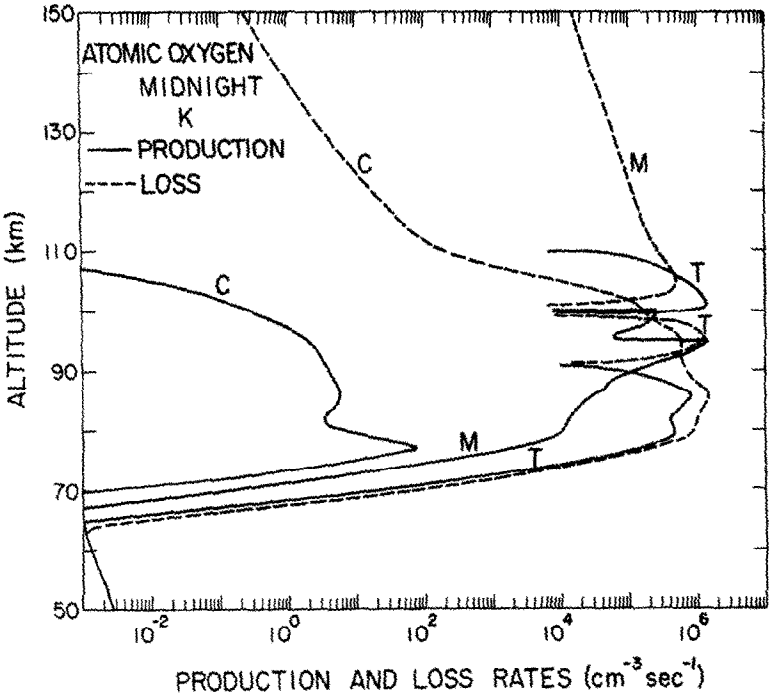

FIG. 8. SAME AS FIG. 7 EXCEPT FOR MIDNIGHT.

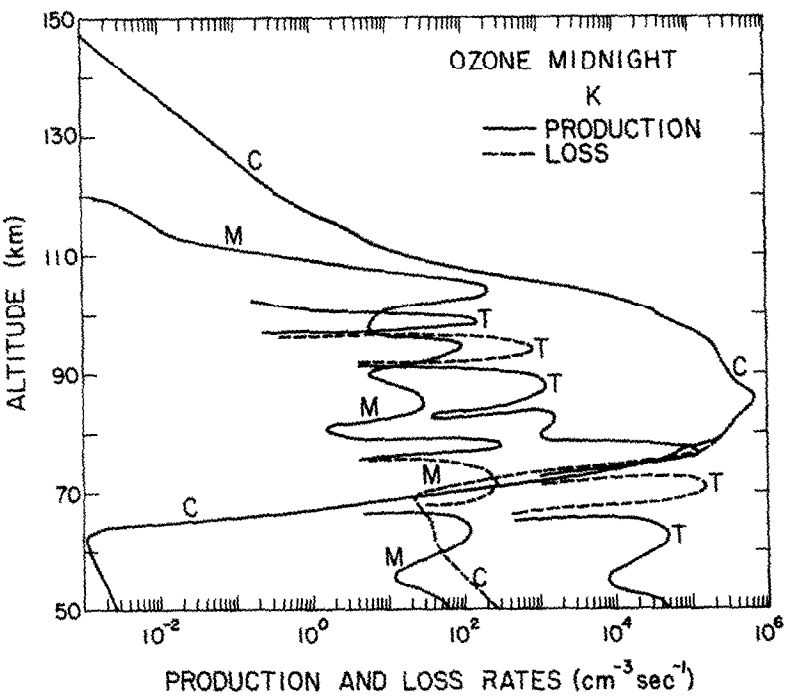

FIG. 9. SAME AS FIG. 8 EXCEPT FOR OZONE.

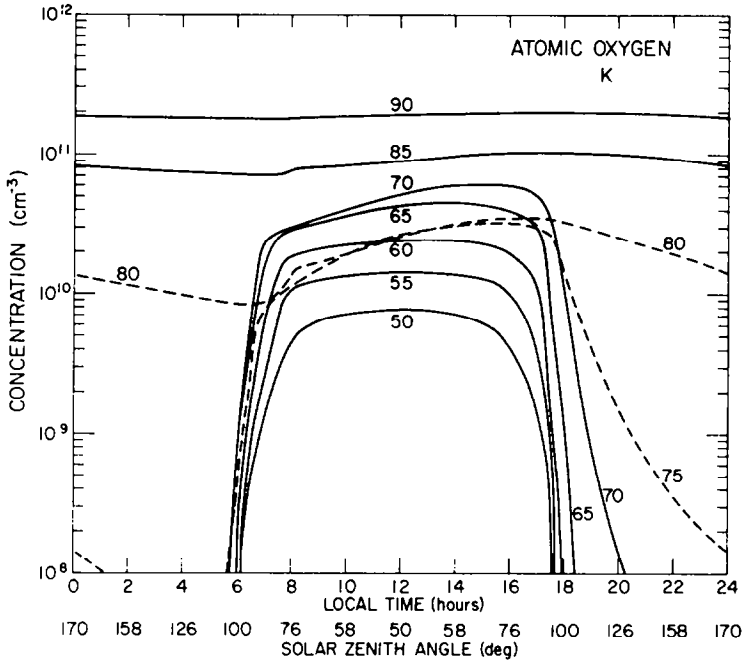

FIG. 10. DIURNAL VARIATION OF ATOMIC OXYGEN BETWEEN 50 AND 90 km FOR THE K TURBULENT DIFFUSIVITY.

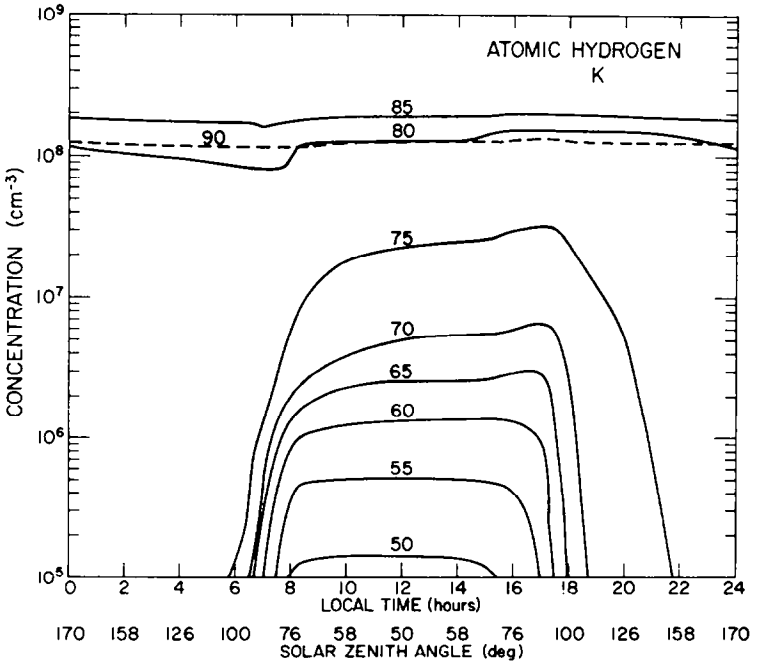

FIG. 11. SAME AS FIG. 10 EXCEPT FOR ATOMIC HYDROGEN.

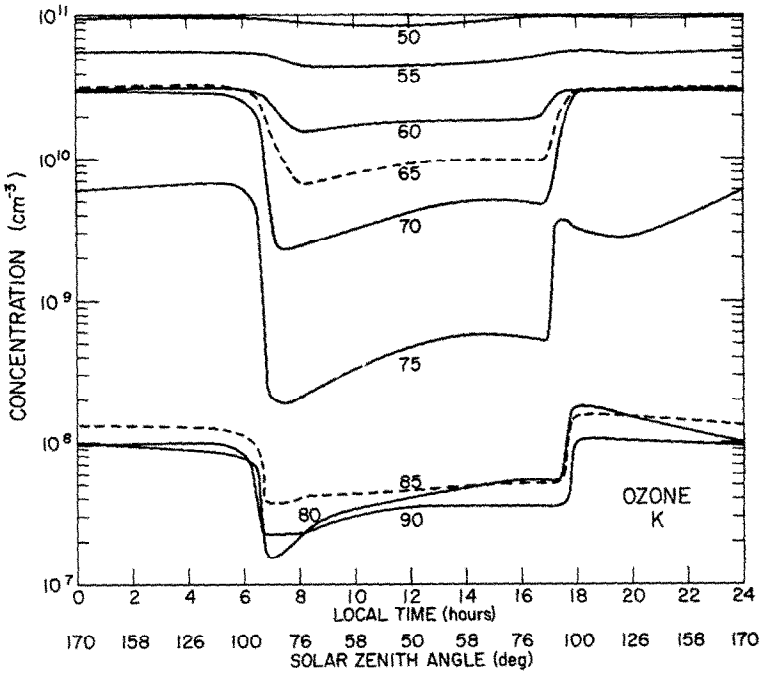

FIG. 12. SAME AS FIG. 11 EXCEPT FOR OZONE.

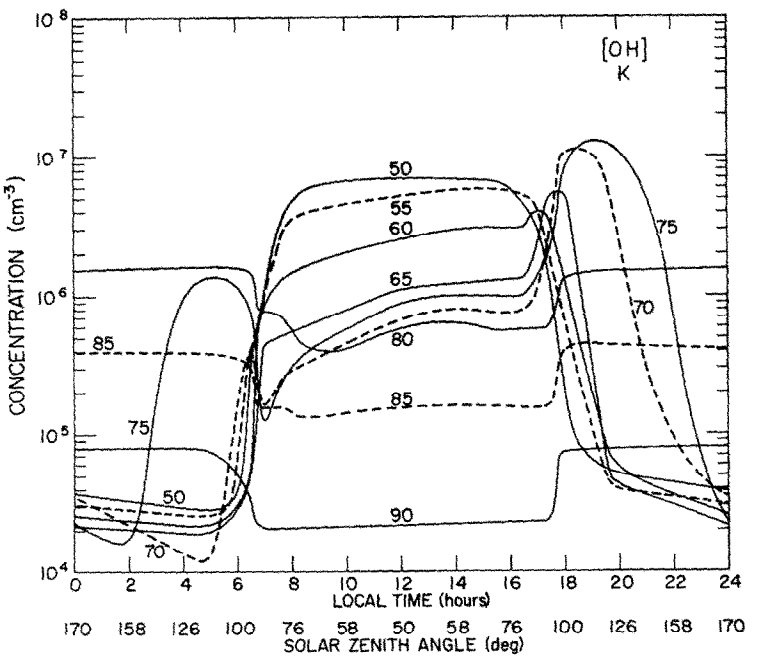

FIG. 13. SAME AS FIG. 11 EXCEPT FOR THE HYDROXYL RADICAL.

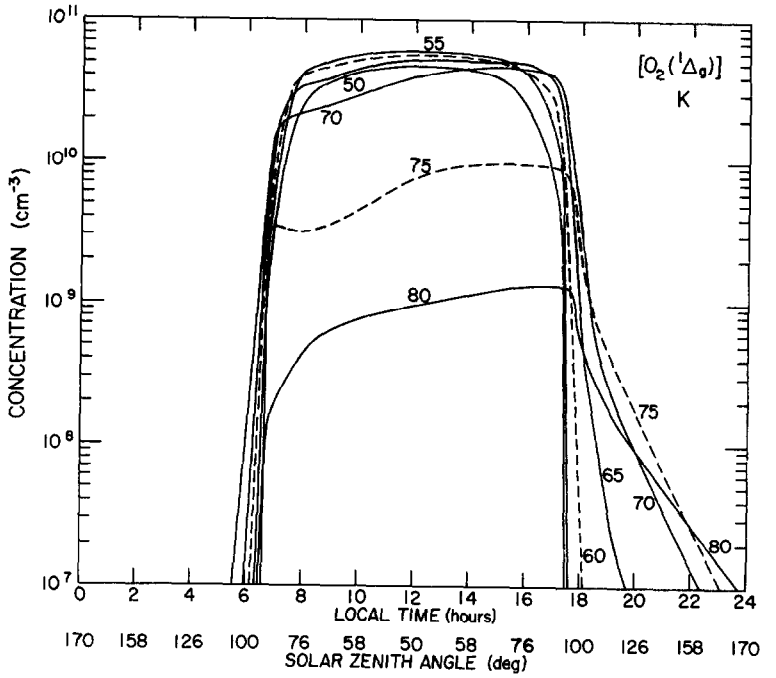

FIG. 14. SAME AS FIG. 11 EXCEPT FOR $O_2(^1\Delta_g)$.

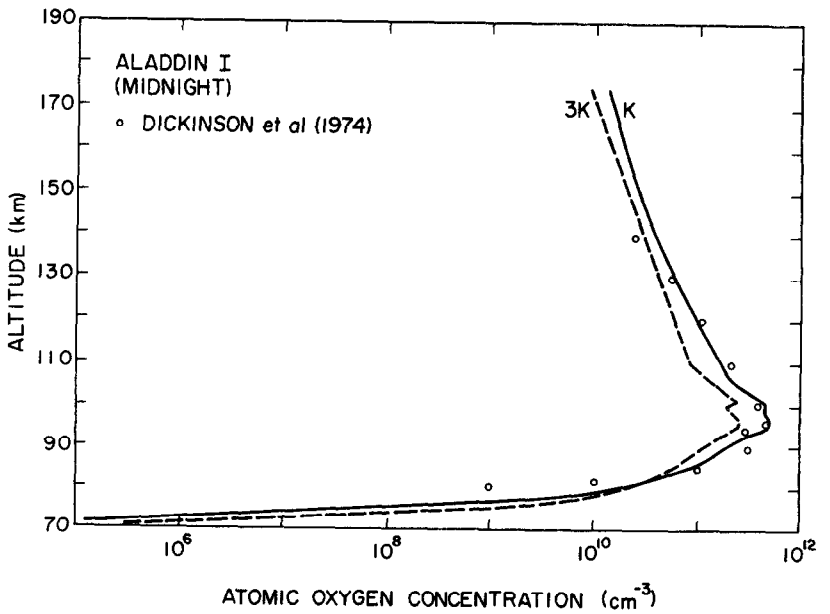

FIG. 15. COMPARISON OF THE MIDNIGHT ATOMIC OXYGEN PROFILES WITH MEASUREMENTS OF DICKINSON *et al.*, (1974).

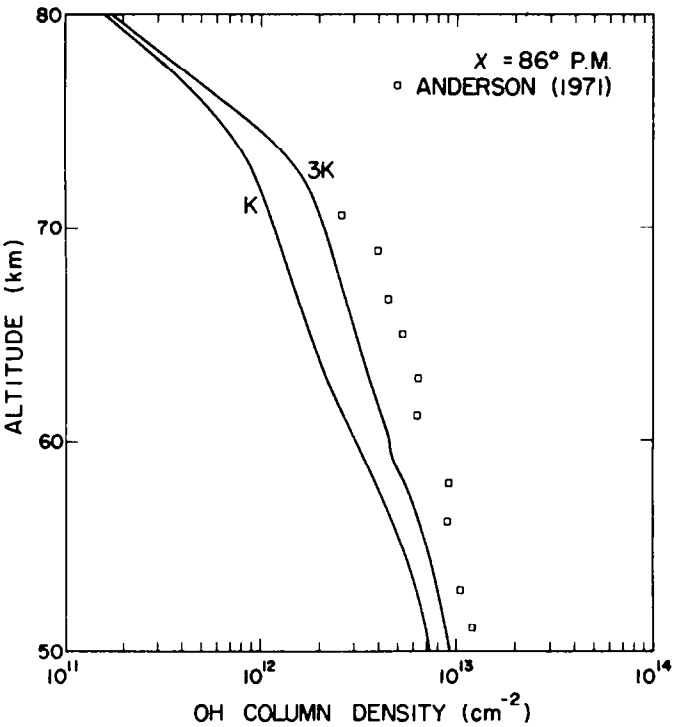

FIG. 16. COMPARISON OF THE INTEGRATED HEIGHT PROFILES OF OH AT A SOLAR ZENITH ANGLE OF 86° WITH THE MEASUREMENT OF ANDERSON (1971).

computed profiles can be chosen at other solar zenith angles for comparison with measurements at other times and locations. One in particular is the reported midnight measurement of atomic oxygen by resonance fluorescence and absorption techniques at South Uist, Scotland (57° 20'N, 7°20'W) at 2237 UT on 1 April 1974 (Dickinson *et al.*, 1974). Figure 15 shows the comparison of these data with the computed midnight atomic oxygen profiles for the K and $3K$ turbulent diffusion coefficients. It may be argued that it is erroneous to compare this model with data taken at a different season, winter for the model calculations and equinox for the Dickinson *et al.*, experiments. However, since the noon solar zenith angles are very close, and since this is a most important factor in the daily production of atomic oxygen, it is felt that the comparison is quite proper. As observed, the correlation between theory and experiment is extraordinarily good over the entire altitude range and particularly near the lower cut-off ledge around 80 km. This is particularly important because of the effect that the turbopause height has upon this species, i.e., the higher the turbopause for a given turbulent intensity, the lower in altitude will be this ledge. This excellent agreement in the night-time cut-off height is another affirmation for the reasoning that the turbulence exhibited in rocket deposited chemical tracer trails in the lower thermosphere is indeed the atmospheric turbulence at these heights and a major transport mechanism.

In Figure 16 is shown a comparison of the model OH profile with the measurement by Anderson (1971) at a solar zenith angle of 86°. The comparison is made with the integrated profile rather than with the reduced concentrations in order to moderate differences created by the differentiation of the measurement. Here, the agreement is fairly good when compared with this measurement, perhaps as good as can be expected considering all the unknown parameters.

In conclusion, it has been demonstrated that a one-dimensional time dependent calculation incorporating measured transport coefficients and the basic state of the atmosphere can reproduce well the simultaneous measurements of the minor species.

Acknowledgement—We wish to express our thanks to the reviewer for suggesting the reaction of H_2O_2 with Cl as a possible loss mechanism for H_2O_2.

REFERENCES

Ackerman, M. (1971). *Ultraviolet Solar Radiation Related to Mesospheric Process in Mesospheric Models and Related Experiments.* (Ed. G. Fiocco), pp. 149–159. D. Reidel, Dordrecht, Netherlands.

Anderson, J. G. (1971). Rocket measurement of OH in the mesosphere. *J. geophys. Res.* **76,** 7820–7824.

Anderson, J. G. and Kaufman, F. (1973). Kinetics of the relation $OH(v=0)+O_3 \rightarrow HO_2+O_2$. *Chem. Phys. Lett.* **19,** 483–486.

Badger, R. A., Wright, A. C. and Whitlock, R. F. (1965). Absolute intensities of the discrete and continuous absorption bands of oxygen gas at 1.26 and 1.065μ and the radiative lifetime of the $^1\Delta_g$ state of oxygen. *J. Chem. Phys.* **43,** 4345–4350.

Banks, P. M. and Kockarts, G. (1973). *Aeronomy, Part A and Part B.* Academic Press, New York.

Baulch, D. L. Drysdale, D. D., Horne, D. G. and Lloyd, A. C. (1972). *Evaluated Kinetic Data for High Temperature Reactions.* Chemical Rubber Company, Cleveland.

Beaudoin, P. E., Golomb, D., Noel, T. M., Rosenberg, N. W. and Vickery, W. K. (1967). Observation of mesosphere winds and turbulence with smoke trails. *J. geophys. Res.* **72,** 3729–3733.

Campbell, I. M. and Thrush, B. A. (1967). The association of oxygen atoms and their combination with nitrogen atoms. *Proc. R. Soc. A,* **296,** 222–232.

Chapman, S. and Cowling, T. G. (1970). *The Mathematical Theory of Non-Uniform Gases.* Cambridge University Press.

Clark, I. D. and Wayne, R. P. (1969). Collisional quenching of $O_2(^1\Delta_g)$. *Proc. R. Soc. A,* **314,** 111–115.

Colegrove, F. D., Hanson W. B. and Johnson, F. S. (1965). Eddy diffusion and oxygen transport in the lower thermosphere. *J. geophys. Res.* **70,** 4931–4941.

Colegrove, F. D., Johnston, F. S. and Hanson, W. B. (1966). Atmospheric composition in the lower thermosphere. *J. geophys. Res.* **71,** 2227–2236.

Davis, D. D., Wong, W. and Schiff, R. (1974). A dye laser flash photolysis kinetics study of the reaction of ground-state atomic oxygen with hydrogen peroxide. *J. Chem. Phys.* **78,** 463–464.

Defense Nuclear Agency, *Reaction Rate Handbook,* (Ed. M. H. Bortner and T. Baurer) General Electric Company-TEMPO, Santa Barbara, California.

Dickinson, P. H. G., Bolden, R. C. and Young, R. A. (1974). Measurement of atomic oxygen in the lower ionosphere using a rocketborne resonance lamp. *Nature,* Lond. **252,** 289–291.

Garvin, D. (1972). Quenching of $O(^1D)$ by water. Chemical Kinetics Data Survey, National Bureau of Standards, Report 10828.

Garvin, D. ed. (1973). Chemical kinetics data survey IV. Preliminary tables of chemical data for modeling of the stratosphere. National Bureau of Standards, Interim Report NDSIR-203.

George, J. D., Zimmerman, S. P. and Keneshea, T. J. (1972). The latitudinal variation of major and minor neutral species in the upper atmosphere. *Space Research XII.* pp. 695–709. Akademie Berlin.

Hampson, R. F., Braun, W. Brown, R. L., Garvin, D., Herron, J. T., Huie, R. E., Kurylo, M. J., Laufer, A. H., McKinley, J. D., Okabe, K. Scheer, M. D., Tsang, W. and Stedman, D. H. (1973). Survey of photochemical and rate data for 28 reactions of interest in atmospheric chemistry. *J. Phys. Chem.* Ref. Data, **2,** 267–311.

Heroux, L. and Swirbalus, R. A. (1976). Full-disk solar fluxes between 1230 and 1940 Å. *J. geophys. Res.* **81,** 436–440.

Hesstvedt, E. (1968). On the effect of vertical eddy transport on atmospheric composition in the mesosphere and lower thermosphere. *Geophys. Norv.* **27,** 1–35.

Hochanadel, C. J., Ghormley, J. A. and Ogren, P. J. (1972). Absorption spectrum and reaction kinetics of the HO_2 radical in the gas phase. *J. Chem. Phys.* **56,** 4426–4432.

Hudson, R. D. and Mahle, S. H. (1972). Photodissociation rates of molecular oxygen in the mesosphere and lower thermosphere. *J. geophys. Res.* **77,** 2902–2914.

Hunten, D. M. and McElroy, M. B. (1970). Production and escape of hydrogen on Mars. *J. geophys. Res.* **75,** 5989–6001.

Hunten, D. M. and Strobel, D. F. (1974). Production and escape of terrestrial hydrogen. *J. atmos. Sci.* **31,** 305-317.

Jacchia, L. G. (1971). Revised static models of the thermosphere and exosphere with empirical temperature profiles. Spec. Rep. 332, Smithson. Astrophys. Observ., Cambridge, MA.

Johnson, F. S. and Wilkins, E. M. (1965). Correction to "Thermal upper limit on eddy diffusion in the mesosphere and lower thermosphere". *J. geophys. Res.* **70,** 4063.

Kaufman, F. (1964). Aeronomic reactions involving hydrogen, a review of recent laboratory studies. *Ann. Geophys.* **20,** 106–114.

Kaufman, F. and Kelso, J. R. (1964). Rate constant of the reaction $O+2O_2 \rightarrow O_3+O_2$. *Discuss. Faraday Soc.* **37,** 26–37.

Kaufman, F. (1969). Neutral reactions involving hydrogen and other minor constituents. *Can. J. Chem.* **47,** 1917–1926.

Keneshea, T. J. and Zimmerman, S. P. (1970). The effect of mixing upon atomic and molecular oxygen in the 70–170 km region of the atmosphere. *J. atmos. Sci.* **27,** 831–840.

Lake, L. R., Nier, A. D. (1973). Loss of atomic oxygen in mass spectrometer ion sources. *J. geophys. Res.* **78,** 1645–1653.

Lettau, H. (1951). Diffusion in the upper atmosphere. Compendium of Meteorology, Boston, Amer. Meteor. Soc., 320–333.

Lumley, J. L. (1964). The spectrum of nearly inertial turbulence in a stably stratified fluid. *J. atmos. Sci.* **21,** 99–102.

Philbrick, C. R., Narcisi, R. S., Good, R. E., Hoffman, H. S., Keneshea, T. J., MacLeod, M. A., Zimmerman, S. P. and Reinisch, B. W. (1973a). The ALADDIN experiment-part II, composition. *Space Research XIII.* pp. 441–448. Akademie Berlin.

Philbrick, C. R., Foucher, G. A. and Trzcinski, E. (1973b). Rocket measurements of megospheric and lower thermospheric composition. *Space Research XIII.* pp. 255–260. Akademie Berlin.

Phillips, O. M. (1967). On the Bolgiano and Lumley–Shur theories of the buoyancy subrange. Atmospheric Trublence and Radiowave Propagation. Nauka, Moscow, USSR.

Richtmyer, R. D. and Morton, K. W. (1967). *Difference Methods for Initial-Value Problems.* pp. 198–201. Interscience, New York.

Rosenberg, N. W., Golomb, D., Zimmerman, S. P., Vickery, W. K. and Theon, J. S. (1973). The ALADDIN experiment-part I, dynamics, *Space Research XIII.* pp. 435–439. Akademie, Berlin.

Schiff, H. I. (1969). Neutral reactions involving oxygen and nitrogen. *Can. J. Chem.* **47,** 1903–1916.

Schmidt, C. and Schiff, H. I. (1973). Reactions of $O_2(^1\Delta_g)$ with atomic nitrogen and hydrogen. *Chem. Phys. Lett.* **23,** 339–342.

Shimazaki, T. (1967). Dynamic effects on atomic and molecular oxygen density distributions in the upper atmosphere: a numerical solution to equations of motion and continuity. *J. atmos. terr. Phys.* **29,** 723–747.

Shimazaki, T. and Laird, A. R. (1970). A model calculation of the diurnal variation in minor neutral constituents in the mesosphere and lower thermosphere including transport effects. *J. geophys. Res.* **74,** 4055–4063.

Snelling, D. F. and Bair, E. J. (1967). Nonadiabatic decomposition of N_2O in the deactivation of $O(^1D)$ by N_2. *J. Chem. Phys.* **47,** 228-234.

Strobel, D. F. (1972). Minor neutral constituents in the mesosphere and lower thermosphere. *Radio Sci.* **7,** 1–21.

Theon, J. S. and Horvath, J. J. (1972). ALADDIN neutral atmosphere measurements. *Trans. Am. geophys. Un.* **53,** 463.

U.S. Standard Atmosphere Supplements (1966). U.S. Government Printing Office, Washington, D.C.

Volman, D. H. (1963). Photochemical gas phase reactions in the hydrogen–oxygen system. *Advances in Photochemistry.* Vol. 1 pp. 43–82 (Eds. Noyes, W. A., G. S. Hammond and J. N. Pitts), Interscience, New York.

von Zahn, U. (1970). Neutral air density and composition at 150 kilometers. *J. geophys. Res.* **75,** 5517–5527.

Watanabe, K. and Zelikoff, M. J. (1953). Absorption coefficients of water vapor in the vacuum ultra violet. *J. Opt. Soc. Am.* **43,** 753–755.

Wayne, R. P. and Pitts, J. N., Jr. (1969). Rate constant for the reaction $O_2(^1\Delta_g) + O_3 \rightarrow 2O_2 + O$. *J. Chem. Phys.* **50,** 3644–3645.

Wong, E. L. and Potter, A. E. (1965). Mass-spectrometric investigations of the reactions of O atoms with H_2 and NH_3. *J. Chem. Phys.* **43,** 3371–3382.

Young, R. A., Black, G. and Slanger, T. G. (1968). Reaction and deactivation of $O(^1D)$. *J. Chem. Phys.* **49,** 4758–4768.

Zimmerman, S. P. and Champion, K. S. W. (1963). Transport processes in the upper atmosphere. *J. geophys. Res.* **68,** 3049–3056.

Zimmerman, S. P. and Trowbridge, C. A. (1973). The measurement of turbulent spectra and diffusion coefficients in the altitude region 95 to 110 km. *Space Research* XIII, 203–208. Akademie, Berlin.

Zimmerman, S. P. and Keneshea, T. J. (1976). The thermosphere in motion. *J. geophys. Res.* **81,** 3187–3197.